Journal of Applied Analysis and Computation
Volume 8, Number 6, December 2018, 1645–1663
Website:http://jaac.ijournal.cn
DOI:10.11948/2018.1645

LATTICE BOLTZMANN MODEL FOR TWO-DIMENSIONAL GENERALIZED SINE-GORDON EQUATION*

Yali Duan[1,†], Linghua Kong[2], Xianjin Chen[1], and Min Guo[3]

Abstract The nonlinear sine-Gordon equation arises in various problems in science and engineering. In this paper, we propose a numerical model based on lattice Boltmann method to obtain the numerical solutions of two-dimensional generalized sine-Gordon equation, including damped and undamped sine-Gordon equation. By choosing properly the conservation condition between the macroscopic quantity u_t and the distribution functions and applying the Chapman-Enskog expansion, the governing equation is recovered correctly from the lattice Boltzmann equation. Moreover, the local equilibrium distribution function is obtained. The numerical results of the first three examples agree well with the analytic solutions, which indicates the lattice Boltzmann model is satisfactory and efficient. Numerical solutions for cases involving the most known from the bibliography line and ring solitons are given. Numerical experiments also show that the present scheme has a good long-time numerical behavior for the generalized sine-Gordon equation. Moreover, the model can also be applied to other two-dimensional nonlinear wave equations, such as nonlinear hyperbolic telegraph equation and Klein-Gordon equation.

Keywords Lattice Boltzmann method, Sine-Gordon equation, Chapman-Enskog expansion, soliton.

MSC(2010) 65M99, 65Z05, 74J30, 74S30.

1. Introduction

During the past few decades, the idea of using lattice Boltzmann method (LBM) for numerical solutions of time-dependent partial differential equations (PDEs) [14–18, 30, 36, 39, 40] has received much attention throughout the scientific community. The LBM is based on microscopic models and mesoscopic kinetic equations which is different from the conventional numerical schemes based on discretizations of

†the corresponding author. Email address:ylduan01@ustc.edu.cn(Y. Duan)
[1]School of Mathematical sciences, University of Science and Technology of China, Hefei, Anhui 230026, China
[2]School of Mathematics and Information Science, Jiangxi Normal University, Nanchang, Jiangxi, 330022, China
[3]Department of Basic, North China College of Mechanics and Electrics, Changzhi, Shanxi, 046000, China
*The authors were supported by National Natural Science Foundation of China (Nos. 11101399, 11271171, 11301234) and the Provincial Natural Science Foundation of Jiangxi (Nos. 20161ACB20006, 20142BCB23009, 20151BAB201012).

partial differential equations describing macroscopic conservation laws [2, 8, 24, 31, 34]. The fundamental idea of the LBM is to construct simplified kinetic models that incorporate the essential physics of microscopic or mesoscopic processes, so that the macroscopic averaged properties obey the desired macroscopic equations. Thanks to its advantages in geometrical flexibility, natural parallelity, simplicity of programming and numerical efficiency, the LBM has made great success in many fields and extensively been applied to solving numerous problems.

It has seen a considerable growth in the interest for nonlinear partial differential equations with soliton solutions, such as Korteweg-de Vries [17, 40], Klein-Gordon, and sine-Gordon equations [1, 9, 19], and also some attentions have been paid to models which possess soliton-like structures in higher dimensions [19]. The sine-Gordon equation is known to be a canonical model for a wide variety of physical systems such as separation of two layers of superconducting material by an isolating barrier [26], propagation of magnetic flux in Josephson junctions [10], a unitary theory of elementary particles [11], propagation of ultra-short optical pulses in resonant laser media [38], the vacancy dynamics in a polymer crystal chain [41], the nonlinear dynamics of DNA chain [22], and many others [20].

This paper focused on the numerical computation of the two dimensional time-dependent nonlinear sine-Gordon (SG) equation. Consider two-dimensional sine-Gordon equation:

$$\frac{\partial^2 u}{\partial t^2} + \alpha \frac{\partial u}{\partial t} = \beta \left(\frac{\partial^2 u}{\partial x^2} + \frac{\partial^2 u}{\partial y^2} \right) + \phi(x, y) \sin u + f(u, x, y, t), \tag{1.1}$$

in the region $\Omega = \{(x, y) | a \leqslant x \leqslant b, c \leqslant y \leqslant d\}$. The initial conditions are given by

$$u(x, y, 0) = u_0(x, y), \ \frac{\partial u}{\partial t}(x, y, 0) = v_0(x, y), \quad (x, y) \in \Omega, \tag{1.2}$$

while the boundary conditions associated with Eq.(1) will be assumed to have the forms

$$\frac{\partial u}{\partial x} = p(x, y, t), \ \frac{\partial u}{\partial y} = q(x, y, t) \quad (x, y) \in \Gamma, \ t > 0, \tag{1.3}$$

where $p(x, y, t)$and $q(x, y, t)$are normal gradients along the boundary Γ of the region Ω. The function $\phi(x, y)$ may be interpreted as a Josephson current density and $u_0(x, y)$ and $v_0(x, y)$ represent wave modes or kinks and velocity, respectively. The parameter α is the so-called dissipative term, which is assumed to be a real number with $\alpha \geqslant 0$. When $\alpha = 0$, Eq. (1) reduces to the undamped SG equation in two space variables, while when $\alpha > 0$, to the damped one. For the undamped SG equation in higher dimensions, the exact soliton solutions have obtained by Hirota [25] , Lambs method [12], Painlevé transcendents [28] and Bäcklund transformation [29], etc.

Numerical solutions for the SG equation have given by Djidjeli et al. [19] using a two-step one-parameter leapfrog scheme, Guo et al. [23] using two finite difference schemes, Xin [38] studing sine-Gordon equation as an asymptotic reduction of the two level dissipationless Maxwell-Bloch system, Christiansen and Lomdahl [9] using a generalized leapfrog method and Argyris et al. [1] presenting a semidiscrete Galerkin approach based on simple four-noded bilinear finite elements in combination with a generalized Newmark integration scheme, Sheng et al. [37] by a split cosine scheme, Bratsos [3] using a three time-level fourth-order explicit finite-difference

scheme, Bratsos [4] using a modified predictor-corrector scheme, Bratsos [5] using the method of lines, Bratsos [6] by a third-order numerical scheme. Recently authors of [21] developed the dual reciprocity boundary element method for solving the two-dimensional damped and undamped SG equations. In [33] researchers studied the boundary element solution of two-dimensional SG equation using continuous linear elements approximation. Jiwari et al. [35] proposed a numerical technique based on polynomial differential quadrature method to find the numerical solutions of two-dimensional SG equation with Neumann boundary conditions. In this paper, we present an LBM for the two-dimensional generalized SG equations.

Let $\dfrac{\partial u}{\partial t} = v$, Equations (1.1)-(1.2) can be rewritten in the following form

$$\begin{cases} \dfrac{\partial v}{\partial t} = \beta\left(\dfrac{\partial^2 u}{\partial x^2} + \dfrac{\partial^2 u}{\partial y^2}\right) + R(u,x,y,t), \\ \dfrac{\partial u}{\partial t} = v, \quad R(u,x,y,t) = \phi(x,y)\sin u + f(u,x,y,t) - \alpha v \end{cases} \tag{1.4}$$

with initial conditions

$$\begin{cases} u(x,y,0) = u_0(x,y), \\ v(x,y,0) = v_0(x,y). \end{cases} \tag{1.5}$$

The conservation condition between the macroscopic quantity $\dfrac{\partial u}{\partial t}$ and the distribution functions is chosen properly. The governing equation is recovered correctly from the lattice Boltzmann equation by the Chapman-Enskog expansion with the proper time and space scales, and the local equilibrium distribution function is obtained. Numerical predictions agree well with the analytical solutions and other numerical results.

The paper is organized as follows: Section 2 highlights the lattice Boltzmann model. The application of LBM to the two-dimensional generalized SG equation is presented in the section, and the 5-bit lattice Boltzmann model with second order accuracy of truncation error is obtained. The results of numerical experiments are reported in Section 3. Section 4 is dedicated to a brief conclusion. Finally some references are introduced at the end.

2. Lattice Boltzmann model

According to the theory of the lattice Boltzmann method, it consists of two steps:

(i) colliding, which occurs when particles arriving at a node interact and possibly change their velocity directions according to scattering rules.

(ii) streaming, where each particle moves to the nearest node in the direction of its velocity.

Usually, with the single-relaxation-time or Bhatnagar-Gross-Krook (BGK) [7] approximation, these two steps can be combined into the lattice Boltzmann equation. The evolution equation of the distribution function in the model reads

$$f_i(\mathbf{x} + \mathbf{e}_i\Delta t, t + \Delta t) - f_i(\mathbf{x}, t) = -\frac{1}{\tau}(f_i(\mathbf{x}, t) - f_i^{eq}(\mathbf{x}, t)) + \Delta t\frac{R(\mathbf{x}, u, t)}{b}, \tag{2.1}$$

where $f_i(\mathbf{x},t)$ is the distribution function of particles; $f_i^{eq}(\mathbf{x},t)$ is the local equilibrium distribution function of particles; Δx and Δt are the lattice space and time increments, respectively; $c=\Delta x/\Delta t$ is the particles speed and τ is the dimensionless relaxation time; $\{\mathbf{e}_i, i=0,1,...b-1\}$ is the set of discrete velocity directions and the Roman subscript i is used to label discrete velocities. Here the 5-speed square lattice is used in the present study. The velocity vector of particles is defined by

$$\{\mathbf{e}_i=(e_{ix},e_{iy}), i=0,1,\cdots,4\}=\{(0,0),(c,0),(0,c),(-c,0),(0,-c)\}. \tag{2.2}$$

Consider a lattice with $b-1$ links that connect the center site to $b-1$ neighboring nodes. It is actually a b-bit model if the rest particles with velocity $\mathbf{e}_0=(0,0)$ are allowed at each node. The macroscopic quantity v is defined in terms of the distribution functions as

$$v(\mathbf{x},t)=\frac{\partial u}{\partial t}(\mathbf{x},t)=\sum_i f_i(\mathbf{x},t)=\sum_i f_i^{eq}(\mathbf{x},t). \tag{2.3}$$

To derive the macroscopic equation from the lattice BGK model, the Chapman-Enskog expansion is applied under the assumption of the small Kundsen number ϵ defined as $\epsilon=l/L$, where l is the mean free path, and L is the characteristic length. The Chapman-Enskog expansion is applied to $f_i(\mathbf{x},t)$,

$$f_i=f_i^{eq}+\sum_{n=1}^{\infty}\epsilon^n f_i^{(n)}=f_i^{eq}+\epsilon f_i^{(1)}+\epsilon^2 f_i^{(2)}+\cdots \tag{2.4}$$

and $f_i^{(k)}$ $(k=1,2,...)$ are the nonequilibrium distribution functions, which satisfy the solvability conditions

$$\sum_i f_i^{(k)}=0 \qquad (k=1,2,...). \tag{2.5}$$

In Eq. (2.1), we also assume that $R(u,\mathbf{x},t)$ is the second order term written as

$$R(u,\mathbf{x},t)=\epsilon^2 r(u,\mathbf{x},t). \tag{2.6}$$

Applying the Taylor expansion to the left-hand side of Eq. (2.1) at the point $(\mathbf{x},t)$, we have

$$(\partial_t+\mathbf{e}_i\cdot\nabla_{\mathbf{x}})f_i+\frac{\Delta t}{2}(\partial_t+\mathbf{e}_i\cdot\nabla_{\mathbf{x}})^2 f_i+\cdots=-\frac{1}{\tau\Delta t}(f_i(\mathbf{x},t)-f_i^{eq}(\mathbf{x},t))+\epsilon^2\frac{r(\mathbf{x},u,t)}{b}. \tag{2.7}$$

Introduce the time scales $t_1=\epsilon t, t_2=\epsilon^2 t$, and space scale $\mathbf{x_1}=\epsilon\mathbf{x}$, then the time derivation and the space derivation can be expanded formally:

$$\partial_t=\epsilon\partial_{t_1}+\epsilon^2\partial_{t_2} \quad , \quad \nabla_{\mathbf{x}}=\epsilon\nabla_{\mathbf{x}_1}. \tag{2.8}$$

Substituting Eqs. (2.4), (2.8) into Eq. (2.7) and retaining terms up to $O(\epsilon^3)$, we get the partial differential equations in order of ϵ and ϵ^2:

$$(\partial_{t_1}+\mathbf{e}_i\cdot\nabla_{\mathbf{x}_1})f_i^{eq}=-\frac{1}{\tau\Delta t}f_i^{(1)}, \tag{2.9}$$

$$\partial_{t_2}f_i^{eq}+(\partial_{t_1}+\mathbf{e}_i\cdot\nabla_{\mathbf{x}_1})f_i^{(1)}+\frac{\Delta t}{2}(\partial_{t_1}+\mathbf{e}_i\cdot\nabla_{\mathbf{x}_1})^2 f_i^{eq}=-\frac{1}{\tau\Delta t}f_i^{(2)}+\frac{r(u,\mathbf{x},t)}{b}. \tag{2.10}$$

Taking (2.9) $\times\,\epsilon$ + (2.10) $\times\,\epsilon^2$, summing over i, thus, we have

$$(\epsilon\partial_{t_1}+\epsilon^2\partial_{t_2})(\sum_{i=0}^{b-1}f_i^{eq})+\epsilon\nabla_{\mathbf{x}_1}\cdot(\sum_{i=0}^{b-1}\mathbf{e}_i f_i^{eq})+\epsilon^2\sum_{i=0}^{b-1}(\partial_{t_1}+\mathbf{e}_i\cdot\nabla_{\mathbf{x}_1})f_i^{(1)}$$
$$+\frac{\epsilon^2\Delta t}{2}\sum_{i=0}^{b-1}(\partial_{t_1}+\mathbf{e}_i\cdot\nabla_{\mathbf{x}_1})^2 f_i^{eq}=\sum_{i=0}^{b-1}\epsilon^2\frac{r(u,\mathbf{x},t)}{b}+O(\epsilon^3). \tag{2.11}$$

Using Eqs. (2.3) and (2.9), we get

$$\partial_t v+\nabla_{\mathbf{x}}\cdot(\sum_{i=0}^{b-1}\mathbf{e}_i f_i^{eq})+\Delta t(\frac{1}{2}-\tau)\epsilon^2\sum_{i=0}^{b-1}(\partial_{t_1}+\mathbf{e}_i\cdot\nabla_{\mathbf{x}_1})^2 f_i^{eq}=\sum_{i=0}^{b-1}\epsilon^2\frac{r(u,\mathbf{x},t)}{b}+O(\epsilon^3). \tag{2.12}$$

Let

$$\sum_{i=0}^{b-1}e_{il}f_i^{eq}=0, \tag{2.13}$$

$$\epsilon^2\sum_{i=0}^{b-1}(\partial_{t_1}+\mathbf{e}_i\cdot\nabla_{\mathbf{x}_1})^2 f_i^{eq}=\lambda\triangle u, \tag{2.14}$$

and

$$\sum_{i=0}^{b-1}\epsilon^2\frac{r(u,\mathbf{x},t)}{b}=\sum_{i=0}^{b-1}\frac{R(u,\mathbf{x},t)}{b}=\phi(x,y)\sin u+f(u,x,y,t)-\alpha v, \tag{2.15}$$

where the Roman subscripts l,m denote the Cartesian coordinates x,y.

Applying Eqs. (2.9), (2.13) to Eq. (2.14), we get

$$\begin{aligned}\lambda\triangle u&=\epsilon^2\partial_{t_1}(\sum_{i=0}^{b-1}(\partial_{t_1}+\mathbf{e}_i\cdot\nabla_{\mathbf{x}_1})f_i^{eq})+\epsilon^2\sum_{i=0}^{b-1}\mathbf{e}_i\cdot\nabla_{\mathbf{x}_1}(\partial_{t_1}+\mathbf{e}_i\cdot\nabla_{\mathbf{x}_1})f_i^{eq}\\&=\epsilon\partial_{t_1}\nabla_{\mathbf{x}}\cdot(\sum_{i=0}^{b-1}\mathbf{e}_i f_i^{eq})+\sum_{i=0}^{b-1}(\mathbf{e}_i\cdot\nabla_{\mathbf{x}})^2 f_i^{eq}\\&=\sum_{i=0}^{b-1}(\mathbf{e}_i\cdot\nabla_{\mathbf{x}})^2 f_i^{eq}.\end{aligned} \tag{2.16}$$

Therefore we obtain the second-order moment equation of the local equilibrium distribution from Eq. (2.16)

$$\sum_{i=0}^{b-1}e_{il}e_{im}f_i^{eq}=\lambda u\delta_{lm}. \tag{2.17}$$

Then let

$$\beta=\lambda\Delta t(\tau-\frac{1}{2}), \tag{2.18}$$

the generalized SG (1.1) with the second order accuracy of truncation error is obtained from Eq. (2.12).

Based on Eqs. (2.3), (2.13) and (2.17), the equilibrium distribution functions for 5-bit model are obtained

$$\begin{cases} f_0^{eq} = v - \dfrac{2\lambda u}{c^2}, \\ f_1^{eq} = f_2^{eq} = f_3^{eq} = f_4^{eq} = \dfrac{\lambda u}{2c^2}. \end{cases} \tag{2.19}$$

In the computational process, we apply backward difference to the item $v = \dfrac{\partial u}{\partial t}$ as

$$v(\mathbf{x}, t) = \frac{\partial u}{\partial t}(\mathbf{x}, t) = \frac{u(\mathbf{x}, t) - u(\mathbf{x}, t - \Delta t)}{\Delta t}, \tag{2.20}$$

then using Eq. (2.3), we obtain

$$u(\mathbf{x}, t) = \Delta t \sum_i f_i(\mathbf{x}, t) + u(\mathbf{x}, t - \Delta t). \tag{2.21}$$

3. Numerical results

In this section we present some numerical results of the present scheme introduced above for the two-dimensional generalized SG equation. To illustrate the efficiency of the LBM, we first present several numerical examples, such as breather solution and domain wall collision, in comparison with the exact solutions given in bibliography. Then numerical solutions for various cases involving two dimensional line and ring solitons are also reported.

To measure the difference between the exact solution and numerical solution, we use different error norms for measuring errors. These error norms are defined as:

1. L_∞ error

$$L_\infty = \max_{0 \le i \le n, 0 \le j \le m} \left\{ |u^E(x_i, y_j, t) - u^N(x_i, y_j, t)| \right\}, \tag{3.1}$$

2. The root mean square (RMS) error

$$\mathrm{RMS} = \sqrt{\sum_{i=0}^{n} \sum_{j=0}^{m} \frac{(u^E(x_i, y_j, t) - u^N(x_i, y_j, t))^2}{(n+1)(m+1)}}, \tag{3.2}$$

where the positive integers n and m are the number of the lattice in the x-axis and y-axis direction respectively, $u^E(x_i, y_j, t)$ is the exact solution and $u^N(x_i, y_j, t)$ is the numerical solution at the point (x_i, y_j, t).

3.1. Test problem

Example 3.1. We present some numerical results of 5-bit lattice Boltzmann model for the generalized two-dimensional sine-Gordon equation with homogeneous Dirichlet boundary conditions and initial conditions. To observe the behavior of the nu-

merical method, it was tested on the following problem [13,32]

$$\begin{cases} \dfrac{\partial^2 u}{\partial t^2}+\dfrac{\partial u}{\partial t}=\left(\dfrac{\partial^2 u}{\partial x^2}+\dfrac{\partial^2 u}{\partial y^2}\right)-2\sin u+2\sin[e^{-t}(1-\cos\pi x)(1-\cos\pi y)] \\ \qquad\qquad -\pi^2(\cos\pi x+\cos\pi y-2\cos\pi x+\cos\pi y), \\ u(x,y,0)=(1-\cos\pi x)(1-\cos\pi y), \quad 0\leqslant x,y\leqslant 2, \\ \dfrac{\partial u}{\partial t}(x,y,0)=-(1-\cos\pi x)(1-\cos\pi y), \quad 0\leqslant x,y\leqslant 2, \\ u(0,y,t)=u(2,y,t)=u(x,0,t)=u(x,2,t)=0, \quad 0\leqslant x,y\leqslant 2. \end{cases} \tag{3.3}$$

That is, the domain is $[0,2]\times[0,2]$, and the theoretical solution is taken as $u(x,y,t)=e^{-t}(1-\cos\pi x)(1-\cos\pi y)$. In our numerical results, we let $\Delta x=0.01, \Delta t=0.001$, and $\tau=1$. The errors in the L_∞ norm and root-mean-square (RMS) of errors at different times are given in Table 1. Fig. 1 displays numerical solutions for $t=0.5$ and $t=1$ and also shows the graph of absolute error at $t=1$. For this example, Cui [13] proposed a high order compact Alternating Direction Implicit scheme and researchers in [32] developed a space-time spectral method, which is based on the Legendre-Galerkin spectral method in space and the spectral collocation method in time. The numerical results are not better than those obtained in [13,32], because the LBM is of second-order accuracy in space. We can see that the LBM, an unconventional numerical method, is efficient for studying the generalized SG equation.

Table 1. L_∞ norm and RMS of errors at different times.

t	L_∞ error	RMS error	t	L_∞ error	RMS error
0.1	1.1823E–004	5.7123E–005	0.6	2.5382E–003	7.2846E–004
0.2	3.6026E–004	1.6437E–004	0.7	2.8782E–003	8.2492E–004
0.3	8.3158E–004	3.1627E–004	0.8	2.9668E–003	9.1309E–004
0.4	1.4261E–003	4.7358E–004	0.9	2.7847E–003	9.9976E–004
0.5	2.0227E–003	6.1325E–004	1	2.3837E–003	1.0817E–003

3.2. Breather solution and domain wall collision

In the following two experiments, we consider SG equation (1.1) with parameter $\alpha=0$, $\beta=4$ functions $\phi(x,y)=-1$, $f(u,x,y,t)=0$ and the domain $(x,y)\in[-30,30]\times[-30,30]$ That is

$$\frac{\partial^2 u}{\partial t^2}=4\left(\frac{\partial^2 u}{\partial x^2}+\frac{\partial^2 u}{\partial y^2}\right)-\sin u. \tag{3.4}$$

In our numerical experiment, we let $\Delta x=0.2, \Delta t=0.002$, and $\tau=1$. The 5-bit lattice Boltzmann model is tested for the SG equation (3.2) in large domain to show the good long-time numerical behavior.

Example 3.2 (Breather solutions)**.** Breather solutions describe bound pairs of

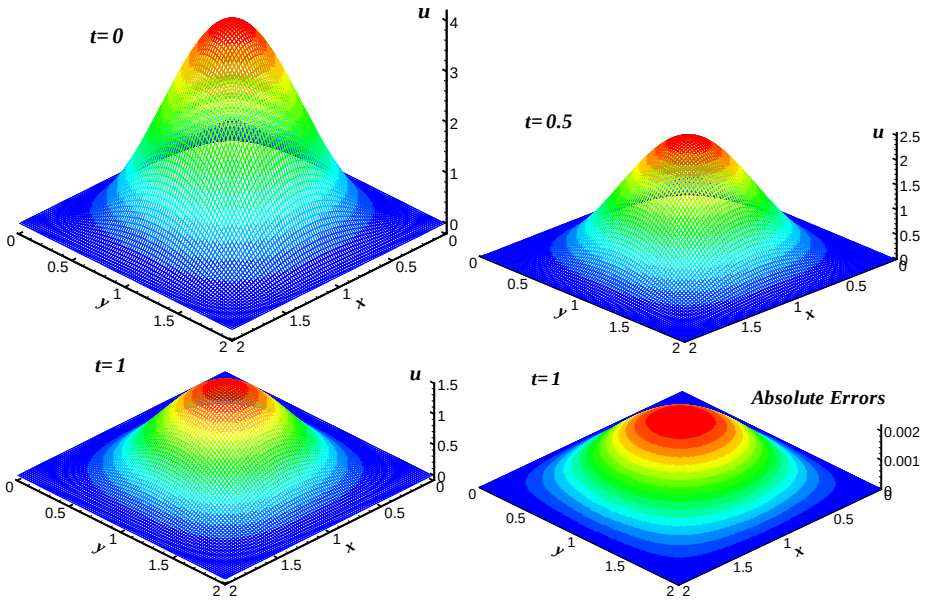

Figure 1. LBM solutions for $t = 0.5$ and $t = 1$ and the absolute error at $t = 1$.

domain walls. Consider SG equation (3.2) with initial conditions

$$\begin{cases} u(x,y,0) = -4\arctan(\operatorname{sech} A \sin B), \\ v(x,y,0) = \dfrac{-2\sqrt{2}\tanh A\ \operatorname{sech} A \sin B + 4\ \operatorname{sech} A \cos B}{1 + \operatorname{sech}^2 A \sin^2 B}, \\ A = \dfrac{\sqrt{2}}{4}(x+y), \quad B = \dfrac{1}{4}(x+y). \end{cases} \tag{3.5}$$

The analytical solution of this example is given in [27] by

$$u(x,y,t) = 4\arctan\left(\sin(t - 0.25x - 0.25y)\ \operatorname{sech}\left(\frac{\sqrt{2}}{4}(2t - x - y)\right)\right). \tag{3.6}$$

L_∞ and RMS errors are computed for different values of t and reported in Table 2 with $\Delta x = 0.2$, $\Delta t = 0.002$, and $\tau = 1$. Fig. 2 displays the simulation of the breather solution with the LBM in times $t = 5, 7$ and 10.

Table 2. L_∞ and RMS errors of solutions for the breather solution at different times.

Error	t=1	t=3	t=5	t=7	t=10
L_∞	4.2579E–003	1.3424E–002	2.6397E–002	3.1883E–002	5.8423E–002
RMS	6.3971E–004	1.9192E–003	3.5543E–003	4.6949E–003	6.1691E–003

Example 3.3 (Domain wall collision)**.** Consider SG equation (3.2) with initial

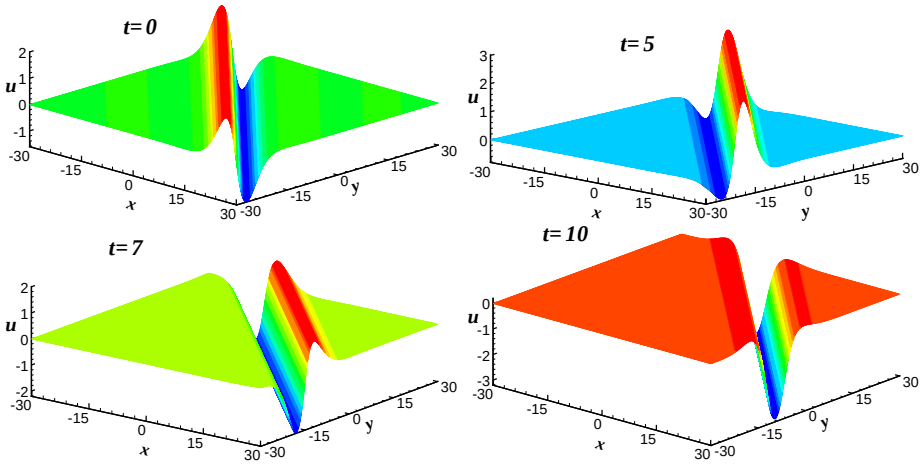

Figure 2. LBM solutions for the breather solution at $t = 5, 7$ and 10.

conditions

$$\begin{cases} u(x,y,0) = -4\arctan(1.5\ \mathrm{sech}A\sinh B), \\ v(x,y,0) = \dfrac{-3.6\sqrt{5}\tanh A\ \mathrm{sech}A\sinh B + 2.4\sqrt{10}\ \mathrm{sech}A\cosh B}{1 + 2.25\ \mathrm{sech}^2 A\sinh^2 B}, \\ A = \dfrac{3\sqrt{5}}{10}(x+y), \quad B = \dfrac{1}{\sqrt{10}}(x+y). \end{cases} \tag{3.7}$$

The analytical solution of this example is given in [27] by

$$u(x,y,t) = 4\arctan\left(1.5\sinh\left(\frac{\sqrt{10}}{10}(4t-x-y)\right)\ \mathrm{sech}\left(\frac{3\sqrt{5}}{10}(2t-x-y)\right)\right). \tag{3.8}$$

Table 3 shows the L_∞ and RMS errors in solutions for different times $t = 1, 3, 5, 7, 10$. Fig. 3 displays the simulation of collision of two domain walls with th LBM at $t = 5, 7$ and 10. In this example, we also see that the LBM is an efficient method for studying the SG equation with collision of two waves.

Table 3. L_∞ and RMS errors of solutions for the domain wall collision at different times.

Error	t=1	t=3	t=5	t=7	t=10
L_∞	2.0837E–002	4.4434E–002	5.1090E–002	4.9758E–002	4.8267E–002
RMS	1.8736E–003	3.8194E–003	5.2179E–003	6.0985E–003	6.6005E–003

In all the following experiments, the Neumann boundary conditions are taken to be

$$\frac{\partial u}{\partial x}|_\Gamma = 0, \quad \frac{\partial u}{\partial y}|_\Gamma = 0, \tag{3.9}$$

and parameter $\beta = 1$, function $f(u,x,y,t) = 0$.

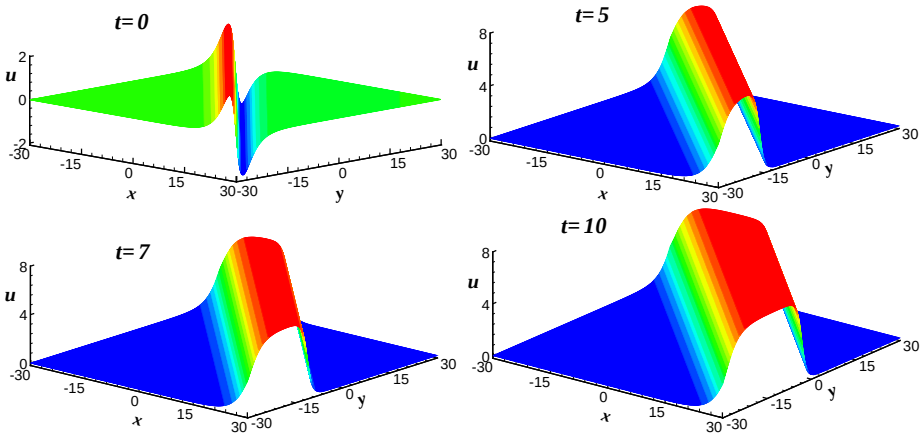

Figure 3. LBM solutions for the domain wall collision at $t = 5, 7$ and 10.

3.3. Line soliton

Example 3.4 (Perturbation of a line soliton)**.** A static line soliton is perturbed to produce two symmetric dents moving towards each other with a constant unit velocity. According to [1, 5, 9, 21], the dents collide and continue with the same velocity and no shift occurs. Perturbation of a single soliton has been calculated for $\alpha = 0.05$ and $\phi(x, y) = -1$ with the initial conditions

$$u(x, y, 0) = 4 \arctan\{\exp[x + 1 - 2 \operatorname{sech}(y + 7) - 2 \operatorname{sech}(y - 7)]\}, \quad v(x, y, 0) = 0,$$

over the region $-7 \leqslant x, y \leqslant 7$. Perturbation of a single soliton has been depicted in Fig. 4 in terms of $\sin(u/2)$ at $t = 2, 7$ and 11 with $\Delta t = 0.01$, $\Delta x = 0.1$ and $\tau = 1$. The numerical results in Fig. 4 show, two symmetric dents moving toward each other, collapsing at $t = 7$ and continuing to move away from each other thereafter. It can be deduced that after the collision the dents retain their shape, which verifies the conclusions of [1, 5, 9, 21].

Example 3.5 (Line soliton in an inhomogeneous medium)**.** A model for an inhomogeneity on large-area Josephson junction is given by the Josephson current density $\phi(x, y) = -(1 + \operatorname{sech}^2\sqrt{x^2 + y^2})$, and the initial conditions

$$u(x, y, 0) = 4 \arctan\left(\exp\left(\frac{x - 3.5}{0.954}\right)\right), \tag{3.10}$$

$$v(x, y, 0) = 0.629 \operatorname{sech}\left(\exp\left(\frac{x - 3.5}{0.954}\right)\right), \tag{3.11}$$

over the region $-7 \leqslant x, y \leqslant 7$. Numerical results are presented in Fig. 5 for $\alpha = 0.05$ in terms of $\sin(u/2)$ at t=6, 12 and 18 with $\Delta t = 0.01$, $\Delta x = 0.2$ and $\tau = 1$. The results in Fig. 5 show that the line soliton is moving in direction x as a straight line during the transmission through inhomogeneity. As can be seen from Fig. 5 when t tends to 12 a deformation in its straightness appears. After t tends to 12 until $t = 18$ this movement seems to be prevented, while when $t = 18$ the soliton recovers its straightness. Christiansen and Lomdahl [9], claimed that this was due

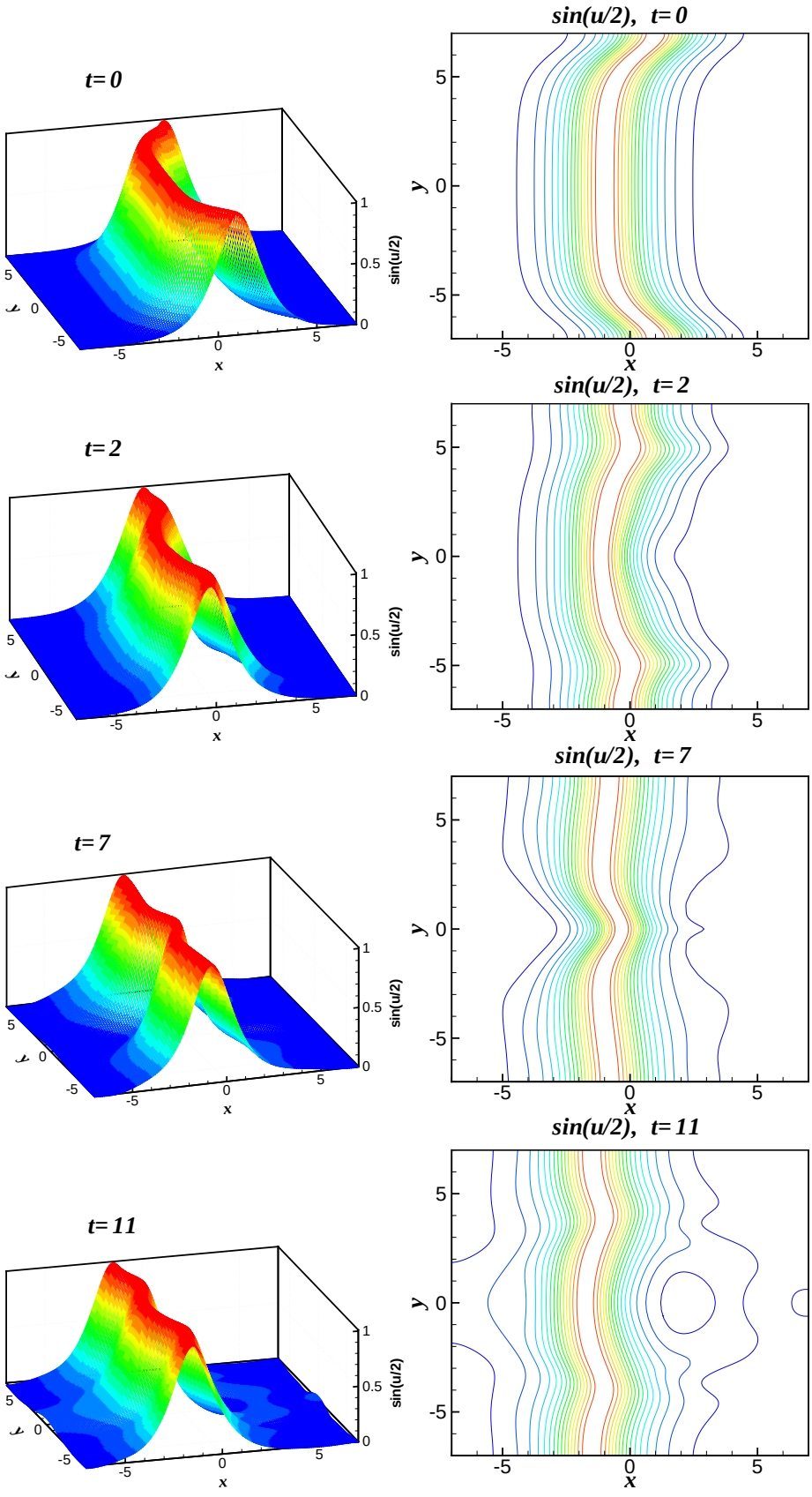

Figure 4. Initial condition and numerical solutions at times $t = 2, 7$ and 11 for perturbation of a line soliton.

to the boundary conditions used. This phenomenon was observed in [5, 9, 19, 21]. For a large value of α, transmission of the line soliton across inhomogeneity was found to hardly move the soliton from its initial position ($t = 0$), the dissipative term is slowing down the evolution of the line soliton as time increases. The graphs are in agreement with those given in [35].

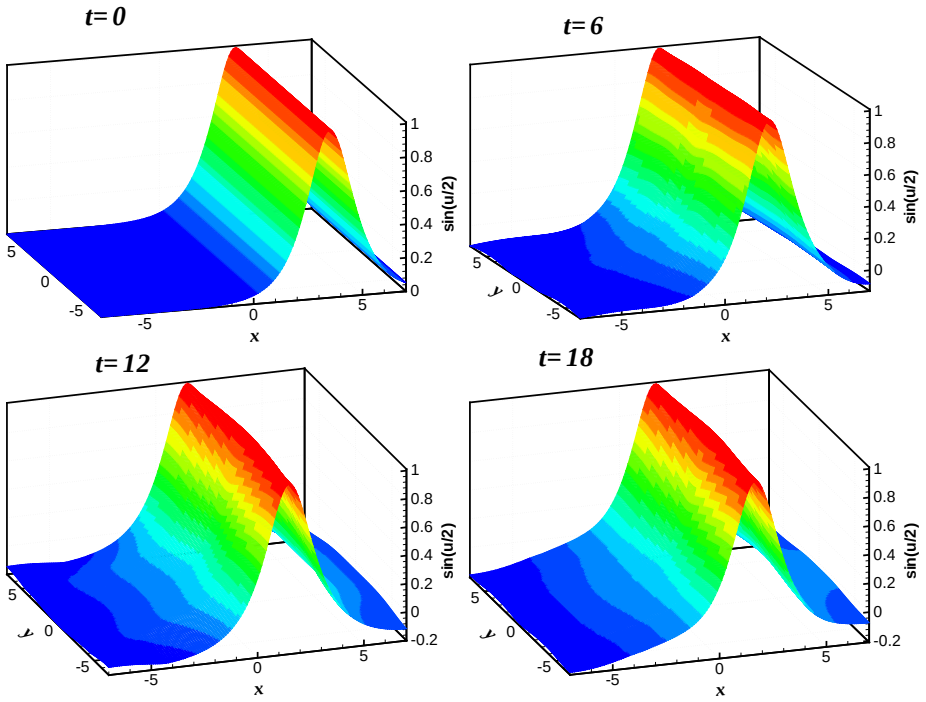

Figure 5. Initial condition and numerical solutions at times $t = 6, 12$ and 18, for line soliton in an inhomogeneous medium.

3.4. Ring soliton

Example 3.6 (Collision of two circular ring solitons)**.** The collision between two circular solitons is considered for $\phi(x, y) = -1$ and initial conditions [19]

$$u(x, y, 0) = 4 \arctan\left(\exp\left(\frac{4 - \sqrt{(x+3)^2 + (y+7)^2}}{0.436}\right)\right), \tag{3.12}$$

$$v(x, y, 0) = 4.13 \operatorname{sech}\left(\exp\left(\frac{4 - \sqrt{(x+3)^2 + (y+7)^2}}{0.436}\right)\right), \tag{3.13}$$

over the region $-30 \leqslant x \leqslant 10$, $-21 \leqslant y \leqslant 7$. The numerical results are presented in Fig. 6 for $\alpha = 0.05$, $\Delta x = 0.2$, $\Delta t = 0.02$ and $\tau = 1$ at $t = 4, 8$ and 11 in terms of $\sin(u/2)$. The solution is extended across $x = -10$ and $y = -7$ by symmetry relations. The results in Fig. 6 show the collision between two expanding circular ring solitons in which, as a result of the collision, two oval ring solitons bounding an annular region emerge into a larger oval ring soliton. For a large value of α, it

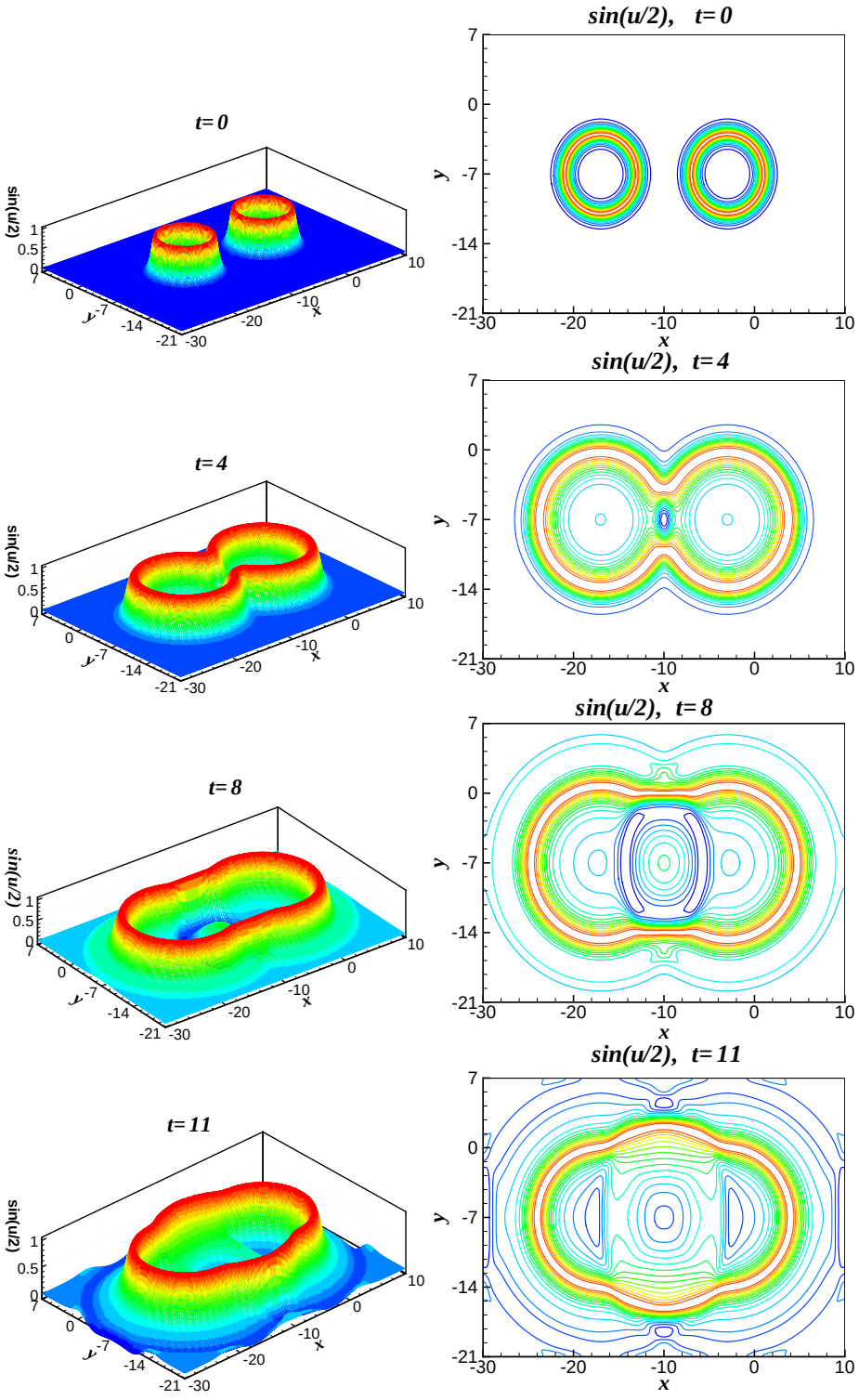

Figure 6. Initial condition and numerical solutions at times $t = 4, 8$ and 11 for collision of two circular ring solitons.

is found that the dissipative term is slowing down the two initial ring solitons to emerge into a larger oval ring soliton. For example, with $\alpha = 5$ the two ring solitons at time $t = 11$ still look like those given at $t = 1.5$ for $\alpha = 0.05$. For see this, we draw the contours of numerical solution at $t = 8$ for $\alpha = 0.05, 0.5, 1.5$, and 2.5 in Fig. 7. The results are in good agreement with those given in [19, 21, 33].

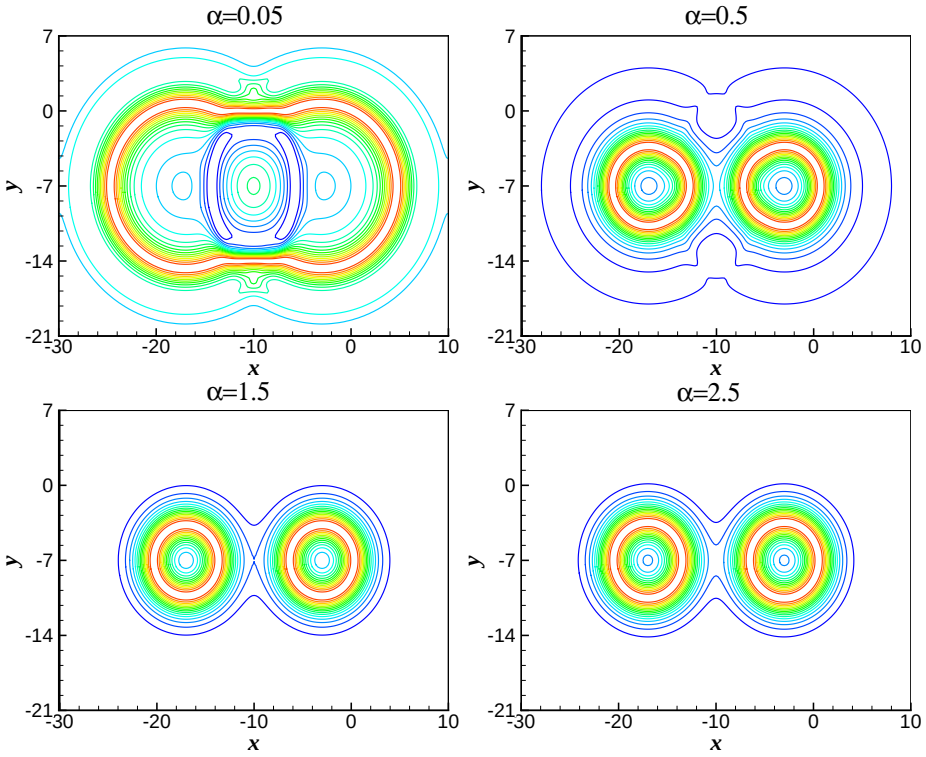

Figure 7. The contours of numerical solutions at time $t = 8$ for $\alpha = 0.05, 0.5, 1.5$ and $\alpha = 2.5$, for collision of two circular ring solitons.

Example 3.7 (Collision of four circular ring solitons)**.** Finally, a collision of four expanding circular ring solitons is investigated for $\phi(x, y) = -1$ and initial conditions [19, 21, 33]

$$u(x, y, 0) = 4 \arctan\left(\exp\left(\frac{4 - \sqrt{(x+3)^2 + (y+3)^2}}{0.436}\right)\right), \tag{3.14}$$

$$v(x, y, 0) = 4.13 \operatorname{sech}\left(\exp\left(\frac{4 - \sqrt{(x+3)^2 + (y+3)^2}}{0.436}\right)\right), \tag{3.15}$$

over the region $-30 \leqslant x, y \leqslant 10$. The solution was found over one-quarter of the domain and then it was extended across $x = -10$ and $y = -10$ by symmetry relations. The numerical results are depicted in Fig. 8 for $\alpha = 0.05$, $\Delta x = 0.2$, $\Delta t = 0.02$ and $\tau = 1$ at $t = 2, 4, 7$ and 9 in terms of $\sin(u/2)$, from which observations similar to those related to the collision of two expanding circular ring solitons may be made.

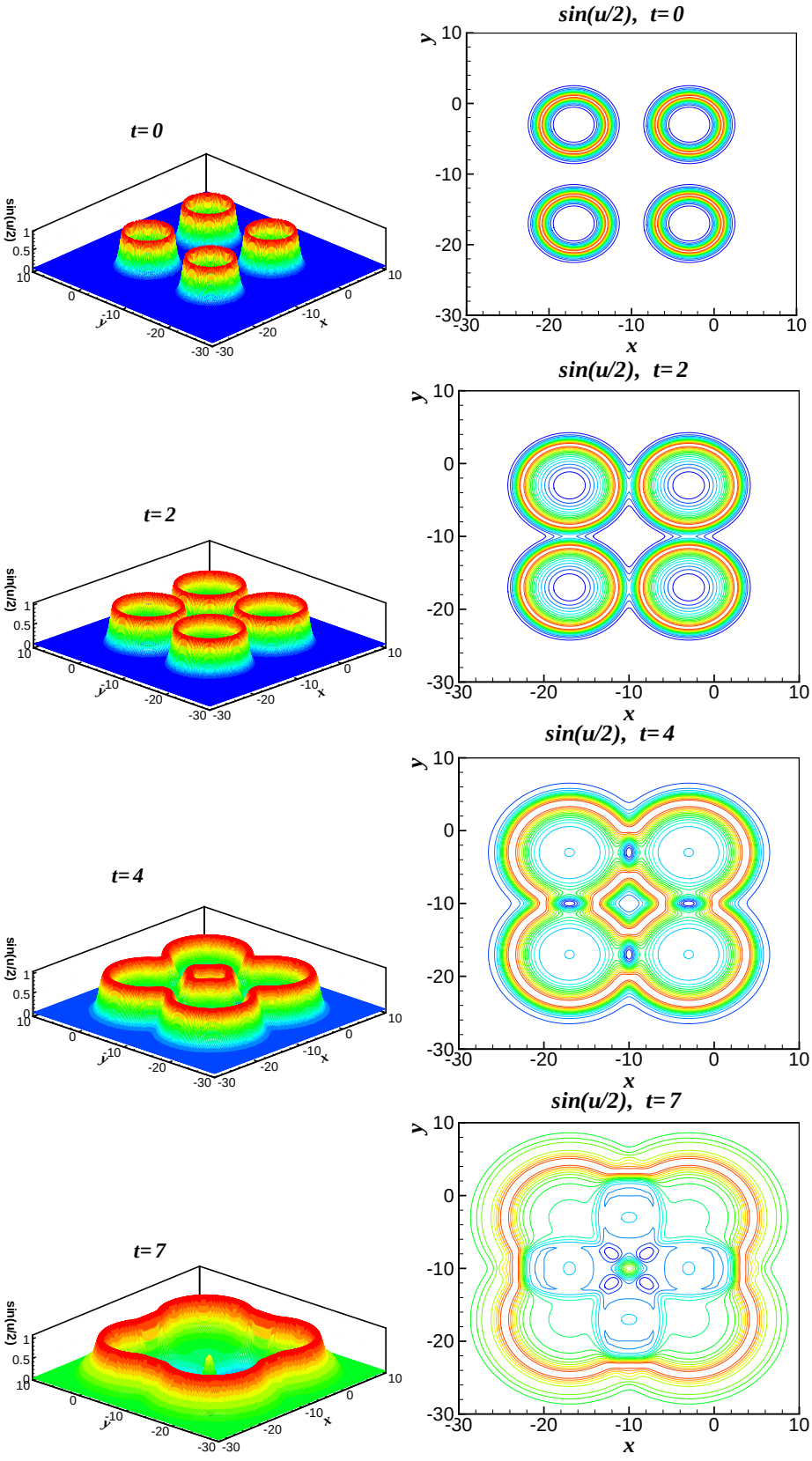
t= 0
sin(u/2), t= 0
t= 2
sin(u/2), t= 2
t= 4
sin(u/2), t= 4
t= 7
sin(u/2), t= 7
sin(u/2)
x
y

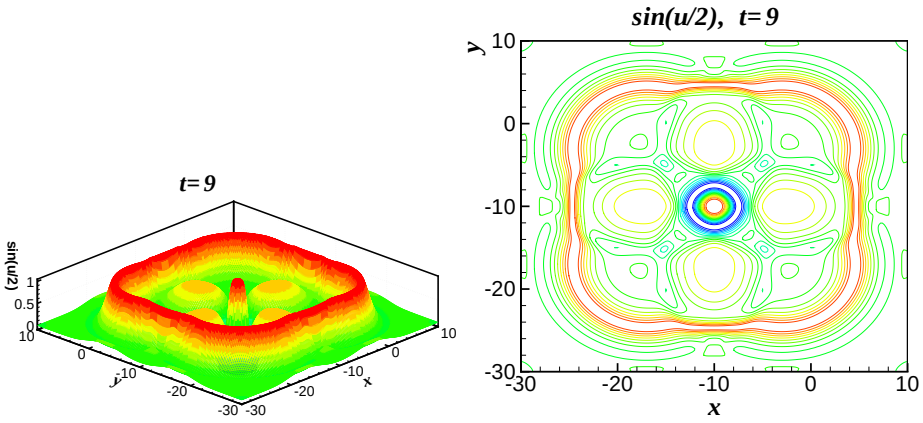

Figure 8. Initial condition and numerical solutions at times $t = 2, 4, 7$ and 9 for collision of four circular ring solitons.

The present method is based on the microscopic model using 5-speed square lattice and mesoscopic kinetic equation (2.1). The model is simple and conservative and it is easy to program. The nonlinear terms can naturally be added to the lattice Boltzmann equation as a source term. It has been seen that, for the case where the exact solution is known, the numerical results demonstrate the numerical efficiency of this scheme. These results supported the confidence in applying this method to problem (1.1) in which the theoretical solution is not known. The effect of the dissipative term in the solution of the sine-Gordon equation has been studied numerically, which corresponds to the physically relevant effect.

4. Conclusions

In this paper, a new lattice Boltzmann model for two-dimensional generalized SG equation is proposed. By choosing properly the conservation condition between the macroscopic quantity u_t and the distribution functions and applying the Chapman-Enskog expansion, the governing equation is recovered correctly from the LBE and the local equilibrium distribution is obtained. In order to illustrate the efficiency of the proposed method, comparisons are made with the exact solutions in the first three examples. It is evident from the numerical section that LBM results are in agreement with the exact solution. Numerical solutions for cases, involving perturbation of a line soliton, line soliton in an inhomogeneous medium, collision of two and four circular ring solitons, are reported. Numerical experiments also show that the present scheme has a good long-time numerical behavior for the generalized SG equation. The method fully satisfies the physical behavior of the nonlinear models.

Finally, we point out that the method in this paper can also be applied to other two-dimensional nonlinear wave equations, such as nonlinear hyperbolic telegraph equation and Klein-Gordon equation. There are many problems to be solved to develop this model as a tool of simulating nonlinear partial differential equation. We would discuss these problems in further work.

Acknowledgements

The authors are very grateful to the reviewers for their valuable comments and suggestions, which have improved the paper.

References

[1] J. Argyris, M. Haase, J. C. Heinrich, *Finite element approximation to two-dimensional sine-Gordon solitons*, Comput. Methods Appl. Mech. Eng., 1991, 86, 1–26.

[2] R. Benzi, S. Succi, M. Vergassola, *The lattice Boltzmann equation: theory and applications*, Phys. Report, 1992, 222(3), 145–197.

[3] A. G. Bratsos, *An explicit numerical scheme for the sine-Gordon equation in 2+1 dimensions*, Appl Numer Anal Comput Math, 2005, 2(2), 189–211.

[4] A. G. Bratsos, *A modified predictor-corrector scheme for the two-dimensional sine-Gordon equation*, Numer Algorithms, 2006, 43, 295–308.

[5] A. G. Bratsos, *The solution of the two-dimensional sine-Gordon equation using the method of lines*, J. Comput. Appl. Math., 2007, 206, 251–277.

[6] A. G. Bratsos, *A third order numerical scheme for the two-dimensional sine-Gordon equation*, Math. Comput. Simulat., 2007, 76, 271–278.

[7] P. Bhatnagar, E. Gross, M. Krook,*A model for collision process in gas. I: Small amplitude processed in charged and neutral one component system*, Phys. Rev., 1954, 94, 511–525.

[8] S. Chen, G. Doolen, *Lattice Boltzmann method for fluid flows*, Annu. Rev. Fluid Mech., 1998, 30, 329–364.

[9] P. L. Christiansen, P. S. Lomdahl, *Numerical solution of 2+1 dimensional sine-Gordon solitons*, Physica D, 1981, 2, 482–494.

[10] J. G. Caputo, L. Loukitch, *Dynamics of point Josephson junctions in a microstrip line*, Physica C: Superconductivity, 2005, 425, 69–89.

[11] T. P. Cheng , L. F. Li, *Gauge Theory of Elementary Particle Physics*, Claendon Press, Oxford, 2000.

[12] P. L. Christiansen, O. H. Olsen, *Return effect for rotationally symmetric solitary wave solutions to the sine-Gordon equation*, Phys Lett A, 1978, 68(2), 185–188.

[13] M. Cui, *High order compact Alternating Direction Implicit method for the generalized sine-Gordon equation*, Journal of Computational and Applied Mathematics, 2010, 235, 837–849.

[14] S. P. Dawson, S. Chen, G. D. Doolen, *Lattice Boltzmann computations for reaction-diffusion equations*, J. Chem. Phys., 1993, 2, 1514–1523.

[15] Y. Duan, R. Liu, *Lattice Boltzmann model for two-dimensional unsteady Burgers' equation*, J. Comput. Appl. Math., 2007, 206, 432–439.

[16] Y. Duan, L. Kong, R. Zhang, *A lattice Boitzmann model for the generalized Burgers-Hulexly equation*, Physics A, 2012, 391, 625–632.

[17] Y. Duan, X. Chen, L. Kong, *Lattice Boltzmann model for the compound Burgers-Korteweg-de Vries equation*, Chin. J. Comput. Phys., 2015, 32(6), 639–648.

[18] Y. Duan, L. Kong, M. Guo, *Numerical simulation of a class of nonlinear wave equations by lattice Boltzmann method*, Commun. Math. Stat., 2017, 5, 13–35.

[19] K. Djidjeli, W. G. Price, E. H. Twizell, *Numerical solutions of a damped Sine-Gordon equation in two space variables*, J. Eng. Math., 1995, 29, 347–369.

[20] Z. Dai, D. Xian, *Homoclinic breather-wave solutions for sine-Gordon equation*, Communications in Nonlinear Science and Numerical Simulation, 2009, 14, 3292–3295.

[21] M. Dehghan, D. Mirzaei, *The dual reciprocity boundary element method (DRBEM) for two-dimensional sine-Gordon equation*, Comput. Methods Appl. Mech. Eng., 2008, 197, 476–486.

[22] J. A. Gonzalez, *M. Martin-Landrove, Solitons in a nonlinear DNA model*, Physics Letters A, 1994, 191, 409–415.

[23] B. Guo, P. J. Pascual, M. J. Rodriguez, L. Vzquez, *Numerical solution of the sine-Gordon equation*, Appl. Math. Comput., 1986, 18, 1–14.

[24] F. Higuera, S. Succi, R. Benzi, *Lattice gas dynamics with enhanced collisions*, Euro. Phys. Lett., 1989, 9, 345–349.

[25] R. Hirota, *Exact three-soliton solution of the two-dimensional sine-Gordon equation*, J Phys Soc Jpn, 1973, 35, 1566.

[26] J. D. Josephson, *Supercurrents through barriers*, Adv. Phys., 1965, 14, 419–451.

[27] S. Johnson, P. Suarez, A. Biswas, *New Exact Solutions for the Sine-Gordon Equation in 2+1 Dimensions*, Computational Mathematics and Mathematical Physics, 2012, 52, 98–104.

[28] P. Kaliappan, M. Lakshmanan Kadomtsev-Petviashvili, *Two-dimensional sine-Gordon equations: reduction to Painlevé transcendents*, J Phys A: Math Gen, 1979, 12, 249–252.

[29] G. Leibbrandt, *New exact solutions of the classical sine-Gordon equation in 2+1 and 3+1 dimensions*, Phys. Rev. Lett., 1978, 41, 435–438.

[30] H. Lai, C. Ma, *Lattice Boltzmann model for generalized nonlinear wave equation*, Phys. Rev. E, 2011, 84, 046708.

[31] L. Luo, *The lattice-gas and lattice Boltzmann methods: past, present and future*, Proceedings of International Conference on Applied Computational Fluid Dynamics. Beijing, China, October, Beijing, 2000, 52–83.

[32] W. Liu, J. Sun, B. Wu, *Space-time spectral method for the two-dimensional generalized sine-Gordon equation*, J. Math.Anal.Appl., 2015, 427, 787–804.

[33] D. Mirzaei, M. Dehghan, *Boundary element solution of the two-dimensional sine-Gordon equation using continuous linear elements*, Engineering Analysis with Boundary Elements, 2009, 33, 12–24.

[34] Y. Qian, S. Succi, S. Orszag, *Recent advances in lattice Boltzmann computing*, Annu. Rev. Comput. Phys., 1995, 3, 195–242.

[35] J. Ram, P. Sapna, R. C. Mittal, *Numerical simulation of two-dimensional sine-Gordon solitons by differential quadrature method*, Computer Physics Communications, 2012, 183, 600–616.

[36] B. Shi, Z. Guo, *Lattice Boltzmann model for nonlinear convection-diffusion equations*, Phy. Rev. E, 2009, 79, 016701.

[37] Q. Sheng, AQM Khaliq, D. A. Voss, *Numerical simulation of two-dimensional sine-Gordon solitons via a split cosine scheme*, Math. Comput. Simulation, 2005, 68, 355–373.

[38] J. Xin, *Modeling light bullets with the two-dimensional sine-Gordon equation*, Physica D, 2000, 135, 345–368.

[39] G. Yan, *A lattice Boltzmann equation for waves*, J. Comput. Phys., 2000, 161, 61–69.

[40] J. Zhang, G. Yan, *A lattice Boltzmann model for the Korteweg-de Vries equation with two conservation laws*, Comput. Phys. Commun., 2009, 180, 1054–1062.

[41] E. A. Zubova, N. K. Balabaev, *Dynamics of soliton-like excitations in a chain of a polymer crystal: influence of neighbouring chains mobility*, Journal of NonlinearMathematical Physics, 2001, 8, 305–311.